AD-A042 764 MINNESOTA UNIV MINNEAPOLIS DEPT OF AEROSPACE ENGINE--ETC F/G 20/11
STRUCTURAL INELASTICITY XIV. AUTOMATIC PIECEWISE LINEARIZATION --ETC(U)
JUN 76 P G HODGE N00014-75-C-0177
UNCLASSIFIED AEM-H1-14 NL

1 OF 1
ADA042 764

END
DATE FILMED
9-77
DDC

Report AEM-H1-14

STRUCTURAL INELASTICITY XIV

Automatic Piecewise Linearization in Ideal Plasticity

Philip G. Hodge Jr., Professor of Mechanics

Department of Aerospace Engineering and Mechanics
University of Minnesota
Minneapolis, Minnesota 55455

June, 1976

Technical Report

Qualified requesters may obtain copies of this report from DDC

Prepared for

OFFICE OF NAVAL RESEARCH
Arlington, VA 22217

OFFICE OF NAVAL RESEARCH
Chicago Branch Office
536 South Clark St.
Chicago, IL 60605

(15) N00014-75-C-0177

SECURITY CLASSIFICATION OF THIS PAGE (When Data Entered)

REPORT DOCUMENTATION PAGE

READ INSTRUCTIONS BEFORE COMPLETING FORM

1. REPORT NUMBER (14) AEM-H1-14	2. GOVT ACCESSION NO.
3. RECIPIENT'S CATALOG NUMBER	
4. TITLE (and Subtitle) STRUCTURAL INELASTICITY XIV. Automatic Piecewise Linearization in Ideal Plasticity.	5. TYPE OF REPORT & PERIOD COVERED Technical Report.
6. PERFORMING ORG. REPORT NUMBER	
7. AUTHOR(s) Philip G. Hodge, Jr., Prof. of Mechanics	8. CONTRACT OR GRANT NUMBER(s) N00014-75-C-0177
9. PERFORMING ORGANIZATION NAME AND ADDRESS University of Minnesota Minneapolis, Minnesota 55455	10. PROGRAM ELEMENT, PROJECT, TASK AREA & WORK UNIT NUMBERS NR 064-429
11. CONTROLLING OFFICE NAME AND ADDRESS OFFICE OF NAVAL RESEARCH Arlington, VA 22217	12. REPORT DATE (11) June 1976
	13. NUMBER OF PAGES 42 (12) 45 p.
14. MONITORING AGENCY NAME & ADDRESS (if different from Controlling Office) OFFICE OF NAVAL RESEARCH Chicago Branch Office 536 South Clark St. Chicago, IL 60605	15. SECURITY CLASS. (of this report) Unclassified
	15a. DECLASSIFICATION/DOWNGRADING SCHEDULE

16. DISTRIBUTION STATEMENT (of this Report)

Qualified requesters may obtain copies of this report from DDC

17. DISTRIBUTION STATEMENT (of the abstract entered in Block 20, if different from Report)

18. SUPPLEMENTARY NOTES

19. KEY WORDS (Continue on reverse side if necessary and identify by block number)

Plasticity, piecewise-linear, perfectly-plastic, finite-element method

20. ABSTRACT (Continue on reverse side if necessary and identify by block number)

A method is proposed for constructing a piecewise linear approximation to an arbitrary yield function. The approximation is constructed in the course of solving a given boundary-value problem. Its use is illustrated with some simple examples.

405 395

DD FORM 1 JAN 73 1473 EDITION OF 1 NOV 65 IS OBSOLETE
S/N 0102-014-6601

SECURITY CLASSIFICATION OF THIS PAGE (When Data Entered)

AUTOMATIC PIECEWISE LINEARIZATION IN IDEAL PLASTICITY[1]

by

Philip G. Hodge, Jr.[2]

ABSTRACT

A method is proposed for constructing a piecewise linear approximation to an arbitrary yield function. The approximation is constructed in the course of solving a given boundary-value problem. Its use is illustrated with some simple examples.

1. This research was sponsored by the Office of Naval Research.
2. Russell Severence Springer Visiting Professor, University of California, Berkeley, January-March 1976; permanently Professor of Mechanics, University of Minnesota.

AUTOMATIC PIECEWISE LINEARIZATION IN IDEAL PLASTICITY

1. Introduction. The defining equations of a typical boundary value problem for a linear-elastic/perfectly-plastic material consist of the equilibrium equations

$$\sigma_{ji,j} + F_i = 0 \tag{1}$$

the strain-displacement relations

$$\varepsilon_{ij} = \frac{1}{2}(u_{i,j} + u_{j,i}) \tag{2}$$

and the constitutive equations

$$\dot{\varepsilon}_{ij} = c_{ijk\ell}\dot{\sigma}_{k\ell} + \dot{\lambda}\,\partial f/\partial\sigma_{ij} \tag{3a}$$

$$f \leqslant f_o \qquad \dot{\lambda} \geqslant o \tag{3b,c}$$

$$\text{IF } (f < f_o \text{ OR } \dot{f} < 0) \text{ THEN } \dot{\lambda} = 0 \tag{3d}$$

together with sufficient prescribed boundary conditions on stress or displacement. In Eqs. (3), the yield function f is a given, closed, convex function of the stresses, f_o is a given constant, $c_{ijk\ell}$ are the elastic constants, $\dot{\lambda}$ is an unknown scalar variable, and a superposed dot means differentiation with respect to any time-like parameter.

The usual method of solving this problem is to assume that a complete solution is known at a generic time t_o, to solve the rate problem at t_o, and then to integrate ahead to time $t_o + \Delta t$. The rate problem is defined by the differentiated forms of (1) and (2), together with (3) which may be rewritten as (3a) together with

$$\begin{aligned} &\text{IF } f < f_o \text{ THEN } \dot{\lambda} = 0 \\ &\text{ELSE IF } \dot{f} < 0 \text{ THEN } \dot{\lambda} = 0 \\ &\text{ELSE } (f = 0 \text{ AND } \dot{\lambda} \geqslant 0) \end{aligned} \tag{4}$$

We observe that the first branch in (4) is defined by the known solution at t_o, but that the correct second branch is defined only in terms of the rate solution. Difficulties associated with choosing the correct second branch have been discussed elsewhere [1, 2][3]; here we shall assume that we have already identified the correct branch. Once the rate problem is solved, the stress at time $t_o + \Delta t$ may be written approximately as

$$\sigma_{ij}(t_o + \Delta t) = \sigma_{ij}(t_o) + \Delta t\, \dot{\sigma}_{ij} \tag{5}$$

We are concerned here with the approximation (5) in the case which includes the last branch in (4), $\dot{f} = 0$. If f is a strictly convex function, then it is necessarily non-linear. However, the locus of stress points given by (5) as a function of Δt is a straight line, so that instead of moving along the curved surface $f = f_o$, the stress point moves along a tangent to this surface. As a result, at time $t_o + \Delta t$, f is no longer equal to f_o but is slightly greater than f_o.

This phenomenon is not just the ordinary one associated with using (5) for any nonlinear time dependent problem. Since f is convex, the error is always in one direction, and if no adjustments are made, there is no limit to the resulting value of f_o. In the simple example presented in Sec. 5, an error of up to 20% is easily produced in the load for a given deformation, and a solution is obtained for loads in excess of an upper bound on the yield-point load!

The above argument is based on the premise that f is strictly convex. However, if f is, instead, a piecewise linear yield function, then the problems disappear. So long as plastic flow remains governed by the same set of linear yield functions, then (5) leads to stresses which continue to satisfy $f = f_o$ exactly. Indeed, if we assume that the boundary conditions are piecewise linear in time, then (5) are exact for a certain range of Δt, so that

3. Number in brackets refer to the list of references collected at the end of the paper.

no error at all is introduced by the time integration.

Now, the yield function f is a material property which basically must be determined by experiment. Experimental results will, of course, exhibit scatter due to choice of sample, temperature, previous material history, etc., so that the "true" f is not defined and any f used in problem solving is necessarily approximate. Given this fact, it appears reasonable to choose a piecewise linear approximation because of its computational advantages.

In some simple problems where the principal stress directions are fixed and known, the piecewise linear Tresca yield condition [3] is generally used in preference to the quadratic Mises condition [4]. However, where the principal stress directions are unknown and vary with time, there is no generally accepted piecewise linear yield condition. In this case, the simplest procedure is to regard some simple non-linear criterion such as the Mises yield condition as known to within some degree of accuracy, and then to construct a piecewise linear approximation to within the same accuracy.

In the next two sections we shall describe, first schematically and then in formal detail, a procedure for such a construction which may be carried out simultaneously with a solution of the boundary value problem.
Sections 4 and 5 will present two simple examples to illustrate the method, and the paper will close with a discussion of the limitations of the method and some ideas for its extension.

2. Method. Since the proposed method is particularly useful in obtaining numerical solutions within the framework of a finite element formulation, we shall present it in those terms, but in complete generality otherwise. To this end, consider a generic finite element k of the system

whose stress configuration is described by a finite number of generalized stresses Q_α^k.[4] Let the theoretical non-linear yield condition for element k be $f(Q_\alpha) = f_o$ where f_o is known only to a certain accuracy. Then the only absolute constraints on a theory are that $f \leqslant f_o$ and that the element is elastic for $f < f_o/(1 + \alpha)$ where α defines the uncertainty. For f between these two values, we are free to construct any yield criterion which satisfies the overall requirement of convexity.

Rather than construct the detailed yield condition in advance, we shall construct it in the process of solving the boundary value problem. Before giving details, we discuss the situation schematically in relation to Fig. 1.

The problem is to systematically construct a convex polygon which will lie in the annulus between $f = f_o$ and $f = f_o/(1 + \alpha)$. We shall indicate four possible approaches and show why one of them is preferable.

(1) initial tangent (Fig. 1a). At the point B where the stress trajectory first touches the inner curve, construct a tangent to the inner curve. This method has several drawbacks. If the stress point proceeds along the tangent to the outer curve at point C, then some additional method of construction must be provided to prevent its leaving the outer curve. If the element unloads and reloads then a distinction must be made between D where we should construct a new tangent and E where we would wish to proceed to the already-constructed one.

(b) external tangent (Fig. 1b). At the point where the stress trajectory first touches the outer curve, draw tangents to the inner curve. There is a minor drawback here in that the original trajectory may be outside

4. Since we will be concerned only with the one generic element, we will suppress the superscript k in this section.

of the tangent. However, a more serious objection is that if there are more than two generalized stresses, then the constructed surface is a cone which is not piecewise linear.

(c) backtrack (Fig. 1c). From the point E where the stress trajectory first touches the outer curve, backtrack to D where it most recently was on the inner curve and draw the tangent. This method is some improvement over the initial tangent one, but if the loading now proceeds along the tangent to F it is obvious that some modification must be made.

(d) shrink and back-track (fig. 1d). From the point E with stress coordinates Q'_α where the trajectory first touches the outer curve, find the point F with coordinates $\beta Q'_\alpha$ on the inner curve and draw the tangent. Then backtrack to G where the trajectory most recently crossed this newly-constructed tangent. This method works equally well at H which was reached along a tangent.

Any back-tracking method has a potential hazard in that it is not generally feasible to store the entire trajectory history. Suppose, for example, that when the trajectory reaches the outer curve at W , its history is only available back as far as M which violates the new constraint NP. In that case, instead of constructing the tangent NP to the inner curve, we construct the parallel constraint QR through the point M.

On some later loading the stress trajectory may encounter a previously drawn tangent, in which case plastic flow will be governed by it. For example, along TU the trajectory cannot continue to the outer curve to trigger a new tangent. Rather, it will move along the already established tangent HU.

It appears from this schematic analysis that the shrink and back-track method does not suffer from the drawbacks of the other three, so we shall now

proceed to formalize the procedure.

3. Procedure. We assume without any real loss in generality that the given loads and any prescribed displacements are all piecewise linear in time. If they are first given by explicit non-linear equations these equations can be replaced by piecewise linear approximations before starting the problem. Also, we take the finite element model as given.

Let Q_α^k denote the αth generalized stress in element k, and let $\underset{\sim}{Q}$ be the array of all Q_α^k. Similarly, let $\underset{\sim}{q}$, $\underset{\sim}{p}$, and $\underset{\sim}{u}$ denote, respectively, the arrays of generalized total strain, generalized plastic strain, and generalized displacement.

The total and plastic strain rates are related by

$$\dot{\underset{\sim}{q}} = \underset{\sim\sim}{c}\dot{\underset{\sim}{Q}} + \dot{\underset{\sim}{p}} \tag{6}$$

where $\underset{\sim}{c}$ is the array of elastic constants. If stress, strain, and plastic strain are all initially zero, (6) may be integrated to yield

$$\underset{\sim}{q} = \underset{\sim\sim}{c}\underset{\sim}{Q} + \underset{\sim}{p} \tag{7}$$

and, for the solution of any problem, $\underset{\sim}{u}$ can be determined from $\underset{\sim}{q}$. Therefore, the rate problem need be concerned only with the stress rates $\dot{\underset{\sim}{Q}}$ and plastic strain rates $\dot{\underset{\sim}{p}}$.

For element k, plastic flow will be zero or will be governed by one or more linear yield flats

$$L_j^k \equiv a_{\alpha j}^k \, Q_\alpha^k = 1 \tag{8}$$

where the summation convention applies only to Greek subscripts. At any stage in the solution procedure, a finite number of the L_j^k will be defined, and at the start of the stage each L_j^k will either be equal to one or less than one. Flats with $L_j^k < 1$ will be inactive and flats with L_j^k may be either active with

$$\dot{L}_j^k \equiv a_{\alpha j}^k \, \dot{Q}_\alpha^k = 0 \tag{9}$$

or inactive if

$$\dot{L}_j^k \equiv a_{\alpha j}^k \dot{Q}_\alpha^k < 0 \tag{10}$$

The plastic strain rates in element k are given by

$$\dot{p}_j^k = \Sigma_j' a_{\alpha j}^k \dot{\lambda}_j^k \quad , \quad \dot{\lambda}_j^k \geq 0 \tag{11}$$

where the summation is to be taken only over the active flats in element k.

Equation (6) may be substituted in the compatibility equations to express them as linear relations between $\dot{\underset{\sim}{Q}}$ and $\dot{\underset{\sim}{p}}$, and the $\dot{\underset{\sim}{p}}$ may be replaced by the $\dot{\underset{\sim}{\lambda}}$ from (11). Each active flat will provide an equation in the form (9) and introduce an unknown plastic multiplier $\dot{\lambda}_j^k$. Therefore, for a properly formulated boundary value problem, equilibrium, compatibility, and (9) will provide sufficient linear equations to determine all unknown rates. Although the question of determining which flats are active may be a vexing one, we shall assume that it can be satisfactorily resolved and regard the rate problem as solvable.

The total problem will consist of a finite number of stages. In each stage, the rate problem will first be solved using given values at the beginning of the stage. Next, a number Δt will be obtained which denotes the duration of the stage, and possibly, a new flat may be created for future stages. Finally, values at the end of the stage will be computed to act as initial values for the next stage.

Figure 2 gives a gross outline of the process. We begin with initial values for $\underset{\sim}{Q}$, $\underset{\sim}{p}$, and t. Normally these will be zero, but it might be desirable to begin in the middle of a previously solved problem.

The rate problem is solved including verification that all non-zero $\dot{\lambda}_j^k$ are positive and that all inactive flats where $L_j^k = 1$ satisfy (10).

Next, three numbers are determined. Δt_E is the time remaining until

some exterior requirement forces an end to the stage. This will normally be the end of a linear interval in the initial piecewise linearization of applied loads and displacements, but it may be presented in other terms. Δt_F is defined as the minimum positive time interval over all elements k for the element to reach its nonlinear yield value: $f^k(Q_\alpha^{k\circ} + \Delta t\, \dot{Q}_\alpha^k) = 1$ corresponding to the outer curve in Fig. 1. Finally, Δt_L is defined as the minimum positive time interval over all elements k and over all inactive flats L_j^k for the element to reach the limiting flat value $L_j^k(Q_\alpha^{k\circ} + \Delta t\dot{Q}_\alpha^k) = 1$.

Let the smallest of these three intervals be denoted by Δt^*. If Δt^* is either Δt_E or Δt_L, i.e., if the stage is terminated by either an external cause or a previously defined inactive flat so that all $f^k(Q_\alpha^k) < 1$, then we set $\Delta t = \Delta t^*$ and proceed immediately to ending the stage. However, if $\Delta t^* = \Delta t_F$, then it is necessary to form a new flat and back-track. To this end, let

$$Q_\alpha^{k*} = Q_\alpha^{k\circ} + \Delta t^*\, \dot{Q}_\alpha^k \tag{12}$$

be the stress point responsible for terminating the interval (e.g., point E in Fig. 1d), and define the stress point Q_α^k by

$$Q_\alpha^{k'} = \beta Q_\alpha^* \qquad f(Q_\alpha^{k'}) = 1/(1+\alpha) \tag{13}$$

When f is homogeneous in the generalized stresses, it may be more meaningful to define the inner yield surface by $f^k[(1-\varepsilon)Q_\alpha^k] = 1$ where ε represents the estimated error range in the yield stress. If f is homogeneous of degree n, then the two parameters are related by

$$\varepsilon = 1-(1+\alpha)^{-n} \tag{14}$$

Next a new flat is constructed for element k tangent to the inner surface at $Q_\alpha^{k'}$:

$$(Q_\alpha^k - Q_\alpha^{k'})\, \frac{\partial f}{\partial Q_\alpha^k}\,(Q^{k'}{}_\alpha) = 0 \tag{15}$$

Defining

$$a^k_{\alpha j} = \left[\frac{\partial f/\partial Q^k_\alpha}{Q^k_\beta \partial f/\partial Q^k_\beta}\right]^{Q^{k'}_\alpha} \tag{16}$$

we can rewrite (15) in the form (8). Here j is to be assigned the value $j' + 1$ where j' was the number of the last flat to be constructed for element k.

The interval Δt is now defined by

$$a^k_{\alpha j} \, (Q^{k^\circ}_\alpha + \Delta t \, \dot{Q}^k_\alpha) = 1 \tag{17}$$

so that the stress point lies on the new flat (e.g. point G on trajectory DE in Fig. 1d). If Δt is positive it denotes the end of the stage and we compute the final values. However, if Δt is negative we would have to backtrack into the previous stage, a process which is not generally desirable. In this case, we cancel out the current stage by setting $\Delta t = 0$, but we do add a new flat which will necessarily be active and hence change the rate solution. The new flat is to be parallel to (15) which led to the negative Δt, and is to pass through the point $Q^{k^\circ}_\alpha$ where the stage initiates. Thus, in place of (16) we define

$$a^k_{\alpha j} = \frac{(\partial f/\partial Q^k_\alpha)'}{Q^{k^\circ}_\beta (\partial f/\partial Q^k_\beta)'} \tag{18}$$

where the gradients are still to be evaluated at the original point of inner tangency defined by (13).

With Δt determined under all contingencies, the stage is ended with

$$\begin{aligned} t &= t_o + \Delta t \\ Q_\alpha &= Q^o_\alpha + \Delta t \, \dot{Q}_\alpha \\ p_\alpha &= p^o_\alpha + \Delta t \, \dot{p}_\alpha \end{aligned} \tag{19}$$

strains are computed from (7), and displacements from the strain-displacement relations. Any desired output is generated and the new state is tested to see if the problem is completed. If not, the left-hand sides of (19) are taken as the initial values for the next stage, and the process is repeated.

4. Frame example. As a first example we consider the frame shown in Fig. 3a. The top and bottom bars are rigid,and the top bar is fixed so that the deformation has three degrees of freedom as shown in Fig. 3c; Fig. 3b gives the sign convention for the stress resultants.

We consider a simplified model in which the deformation is confined to hinges at the ends of the bars. Then so long as at least one bar remains elastic, which turns out to be the case up until collapse, the shear forces S_i are all zero, the moments and normal forces at either end of each bar are equal, and $L\eta = \phi/2$ so that the frame has only two degrees of freedom. Further, since conditions in the hinges at either end of a beam are the same, we can carry out the analysis in terms of three elements each representing the hinges in one beam.

Let M_o and N_o be the yield moment and force,respectively, and define dimensionless generalized stresses and a dimensionless load by

$$m_i = M_i/M_o \quad , \quad n_i = N_i/N_o \quad , \quad p = P/N_o \tag{20}$$

Then moment and vertical equilibrium of the lower bar lead to

$$3n_1 + n_2 - n_3 = h(m_1+m_2+m_3) \tag{21a}$$

$$n_1+n_2+n_3 = p \tag{21b}$$

where $h = M_o/LN_o$.

Generalized strains corresponding to m_i and n_i are the slope discontinuity θ_i across the hinge and

$$e_i = N_o u_i / M_o = (1/h)(u_i/L) \tag{22}$$

where u_i is the axial length discontinuity. In terms of the kinematic variables ϕ and δ, the generalized strains are given by

$$\begin{aligned} 2he_1 &= \delta - 3\phi \qquad 2he_2 = \delta - \phi \\ 2he_3 &= \delta + \phi \qquad \theta_1 = \theta_2 = \theta_3 = -\phi/2 \end{aligned} \tag{23}$$

In the numerical example to follow we shall take $h = 0.1$.

As described in [5] the elastic constitutive equations for this simple frame model can only be expressed in terms of an indeterminate magnitude constant which represents a scale factor for the displacement configuration. Without loss of generality, we take this constant to be unity, whence with $h = 0.1$ the elastic rate equations can be written

$$\begin{aligned} \dot{n}_1 &= 2.5(\dot{\delta} - 3\dot{\phi}) \qquad \dot{n}_2 = 2.5(\dot{\delta} - \dot{\phi}) \\ \dot{n}_3 &= 2.5(\dot{\delta} + \dot{\phi}) \qquad \dot{m}_1 = \dot{m}_2 = \dot{m}_3 = -\dot{\phi}/3 \end{aligned} \tag{24}$$

In order to illustrate a variety of loading behavior, we shall choose the yield stresses shown in circles in Fig. 3a for the three bars as in Drucker's truss [6]. Then the yield curves each consist of two parabolas:

$$\begin{aligned} f_1^{\pm} &= n^2 \pm m = 1 \qquad f_2^{\pm} = (n/20)^2 \pm m/20 = 1 \\ f_3^{\pm} &= (n/12)^2 \pm m/12 = 1 \end{aligned} \tag{25}$$

Finally, we shall choose the factor α between the inner and outer curves to be 0.1.

If element i is on a single yield flat

$$L_i = an_i + bm_i = 1 \tag{26}$$

then the constitutive equations can be explicitly solved for the generalized stress rates to yield

$$\dot{n}_i = b(2b\dot{e}_i+a\dot{\phi})/(3a^2+4b^2) \qquad \dot{m}_1 = -a\dot{n}_i/b \tag{27}$$

and the condition for continuing plastic flow derived from $\dot{\lambda} \geq 0$ is

$$3a\dot{e}_i-2b\dot{\phi} \geq 0 \tag{28}$$

When element i stays on two independent flats of the form (26), the only solution is $\dot{n}_i = \dot{m}_i = 0$ in place of (27). In this case, the inequality (28) must be satisfied for both flats.

We consider the behavior of the frame as P is slowly increased until collapse occurs. It is convenient to take δ (which is monotonically increasing under increasing P) as the time variable, whence the load is determined by Eq. (21b).

All elements are elastic in the first stage, which ends at $\delta_F = 1.963$ when $f_1^- = 1$ with $(n_1, m_1) = (0.907, -0.178)$. The corresponding shrunk point is $\beta(n_1, m_1)$ where β is the solution of

$$(0.907\beta)^2 + (0.178\beta) = 1/1.1 \tag{29}$$

which leads to $(n_1', m_1') = (0.860, -0.169)$. The tangent line to the inner yield curve at this point is

$$L_{11} = 1.043n_1-0.606m_1 = 1 \tag{30a}$$

and, repeating the elastic solution, we see that the limiting value is $\delta = 1.863$. Final elastic values for stage 1, which will serve as initial values for stage 2, are recorded on line 1 of Table 1.

In stage 2, element 1 proceeds along L_{11} until it hits the other yield curve $f_1^+ = 1$ at $\Delta\delta_F = 0.394$ with $(n_1, m_1) = (0.934, 0.036)$. Shrinking then leads to the new tangent line

$$L_{12} = 1.049n_1 + 0.561m_1 = 1 \tag{30b}$$

with $\Delta\delta = 0.313$ and the final values recorded in line 2 of Table 2. It is interesting to note that the end value of m_1 is negative even though

$f_1^+ = 1$ was the limiting yield curve.

During stage 3 element 1 remains at the intersection of L_{11} and L_{12}, and the stage limit is determined by element 3 reaching $f_3^- = 1$. This leads to the tangent

$$L_{31} = 0.0874n_3 - 0.0462m_3 = 1 \tag{30c}$$

and the values in line 3 of Table 1.

In stage 4 the frame exhibits behavior similar to Drucker's truss [6] in that element 1 leaves both linear yield faces and unloads elastically. $\Delta\delta_F$ is determined by $f_3^+ = 1$, and

$$L_{32} = 0.0874n_3 + 0.0469m_3 = 1 \tag{30d}$$

For all further loading, element 3 remains at the point $(n_3, m_3) = (11.443, 0.003)$ which is the intersection of L_{31} and L_{32}. At the end of stage 5, during which it is elastic, element 1 yields in compression but with a substantial negative moment: $(n_1, m_1) = (-.677, -.452)$. During stage 6 it yields on

$$L_{13} = -0.995n_1 - 0.724m_1 = 1 \tag{30e}$$

and during stage 7 it leaves L_{13} and moves along

$$L_{14} = -1.049n_1 - 0.557m_1 = 1 \tag{30f}$$

Stage 7 terminates on the tangent

$$L_{15} = -1.057n_1 + 0.563m_1 = 1 \tag{30g}$$

based on $f_1^+ = 1$, and from here on element 1 remains at the intersection of L_{14} and L_{15}.

With both bars 1 and 3 capable of two degrees of freedom in their strain rates, the frame can carry additional load only because of bending strength in bar 2. After a very small increment of load accompanied by large increases of δ and ϕ, bar 2 is restricted by $f_2^- = 1$ and the final tangent plane

$$L_{21} = 0.0503n_2 - 0.0353m_2 = 1 \tag{30h}$$

If the load is maintained at the value p = 25.484, then a solution exists with all stress rates equal to zero and $\dot{\delta} = \dot{\phi}$ being any positive number. Therefore, collapse occurs with element 1 on L_{14} and L_{15}, element 2 at a fixed point on L_{21}, and element 3 on L_{31} and L_{32}. Final collapse values are given on line 8 of Table 1. Figure 4 shows the stress trajectories and yield lines of the three elements, and Fig. 5 shows the load-deformation diagrams.

5. Plane stress example. To show that the method works equally simply when there are more than two generalized stresses per element, we consider the simple plane stress example shown in Fig. 6. The triangular plate is fixed along its vertical edge AB and an arbitrary in-plane load is applied at C. We divide the plate into four triangles as shown and assume a linear displacement field in each so that there are six degrees of kinematic freedom described by the nodal displacements. In order to carry out the subsequent analysis in dimensionless terms, we shall take these to be

$$(u_i, v_i) = (2E/L\sigma_o)(U_i, V_i) \qquad i = 1, 2, 3 \tag{31}$$

where U_i, V_i are the physical displacements.

Evidently the strains in triangles 3 and 4 are all equal and $\varepsilon_y^4 = \varepsilon_y^3 = 0$, so that there will be eight generalized strains, defined by

$$2q_1 = 2E\varepsilon_x^1/\sigma_o = u_1 - u_3 \qquad 2q_2 = 2E\varepsilon_y^1/\sigma_o = v_2 - v_3$$

$$2q_3 = 2E\gamma_{xy}^1/\sigma_o = u_2 - u_3 + v_1 - v_3$$

$$2q_4 = 2E\varepsilon_x^2/\sigma_o = u_3 \qquad 2q_5 = 2E\varepsilon_y^2\,\sigma_o = v_2 - v_3 \tag{32}$$

$$2q_6 = 2E\gamma_{xy}^2/\sigma_o = u_2 - u_3 + v_3$$

$$q_7 = 2E\varepsilon_x^3/\sigma_o = 2E\varepsilon_x^4/\sigma_o = u_2 \qquad q_8 = 2E\gamma_{xy}^3/\sigma_o = 2E\gamma_{xy}^4/\sigma_o = v_2$$

The corresponding generalized stresses are the average dimensionless stresses in each triangle. Since constant strains lead to constant stresses for an elastic/perfectly-plastic material, these are simply

$$Q_i = (1/\sigma_o)(\sigma_x^1, \sigma_y^1, \tau_{xy}^1, \sigma_x^2, \sigma_y^2, \tau_{xy}^2, \sigma_x^3, \tau_{xy}^3) \tag{33}$$

Although σ_y^3 is not necessarily zero, it does no work and hence is not a generalized stress; it can always be eliminated from the problem by the constraint $\varepsilon_y^3 = 0$ on the constitutive equations.

The eight Eqs. (32) may be inverted to yield explicit expressions for displacements in terms of strain, and two compatibility relations:

$$u_2 = q_7 \quad v_2 = q_8 \quad u_3 = 2q_4 \quad v_3 = q_8 - 2q_2 \tag{34a}$$

$$u_1 = 2(q_1+q_4) \quad v_1 = 2(q_3+2q_4+q_6-q_7) \tag{34b}$$

$$q_2 - q_5 = 0 \quad 2(q_4+q_5+q_6)-(q_7+q_8) = 0 \tag{34c}$$

For a state of plane stress with $\nu = 1/3$ and $\varepsilon_y^3 = 0$, the constitutive equations (7) may be written

$$\begin{aligned} q_1 &= Q_1 - Q_2/3 + p_1 \quad q_2 = Q_2 - Q_1/3 + p_2 \quad q_3 = 8Q_3/3 + p_3 \\ q_4 &= Q_4 - Q_5/3 + p_4 \quad q_5 = Q_5 - Q_4/3 + p_5 \quad q_6 = 8Q_6/3 + p_6 \\ q_7 &= 16Q_7/9 + p_7 \quad q_8 = 16Q_8/3 + p_8 \end{aligned} \tag{35}$$

Finally, the equilibrium relations between the generalized stresses are

$$\begin{aligned} Q_3+Q_6+2Q_7 &= 0 \quad Q_2+Q_5+2Q_8 = 0 \\ Q_1+Q_3-Q_4+Q_6 &= 0 \quad Q_2+Q_3+Q_5-Q_6 = 0 \end{aligned} \tag{36}$$

$$Q_1 = 2P_x/\sigma_o \quad Q_3 = 2P_y/\sigma_o \tag{37}$$

We consider a problem in which the tip displacement $u_1 = u$, $v_1 = v$ is prescribed as shown by the heavy curve 1-7 in Fig. 7. Point 7 is determined by the condition $P_y = 0$, and at this point P_x will be negative. The problem is concluded by increasing P_x, through zero, until collapse occurs.

Since, for most of the history, u and v are prescribed, it is convenient to use these as the independent time-like variables. To this end, Eqs. (35) are first substituted in (34) and the results are combined with (36) to provide eight equations for the generalized stresses in terms of u, v, and the plastic strains. It turns out that triangle 3 is always elastic, so that $P_7 = P_8 = 0$ at all times, The resulting equations, written in terms of rates, are displayed in Table 2.

The Mises yield condition is taken for the outer yield surface, hence

$$\begin{aligned} f_1 &= Q_1^2 - Q_1Q_2 + Q_2^2 + 3Q_3^3 \\ f_2 &= Q_4^2 - Q_4Q_5 + Q_5^2 + 3Q_6^2 \\ f_3 &= (7/9)Q_7^2 + 3Q_8^2 \end{aligned} \tag{38}$$

In writing f_3 we have used the elastic relation $\varepsilon_y^3 = \sigma_y - Q_2/3 = 0$ to eliminate σ_y, since triangle 3 never becomes plastic. The inner curve will be defined by a yield stress 95% of σ_o, hence it follows from (14) that $\alpha = .02598$.

We identify eight stages by the numbers in Fig. 7 and use decimal substages to indicate different plastic behavior. In stage 1, $u = 0$, v is decreased to - 2.25, and all elements are elastic. Therefore, all $\dot{p}_i = 0$ and Table 2 immediately gives the stresses in terms of v. The stage terminates externally when $-v = 2.25$.

Stage 2 is initially elastic as u_1 is increased with v_1 held constant, but at $u_F = 2.221$, $f_1 = 1$, with $\underset{\sim}{\sigma}^* \equiv (Q_1, Q_2, Q_3) = (0.847, 0.204, -0.372)$. The associated stress point on the inner curve is $\underset{\sim}{\sigma}' = 0.95\underset{\sim}{\sigma}^*$ and the tangent plane through $\underset{\sim}{\sigma}'$ is

$$L_{11} = 0.784Q_1 - 0.231Q_2 - 1.174Q_3 = 1 \tag{39}$$

Backtracking the elastic solution, we find that stage 2.1 ends with $u=2.055$ with the stress values given on line 2.1 of Table 3.

In stage 2.2, triangle 1 is on L_{11}, hence it follows from (11) and (39) that

$$\begin{aligned} (\dot{p}_1, \dot{p}_2, \dot{p}_3) &= \dot{\lambda}(0.784, -0.231, -1.174) \\ (\dot{p}_4, \dot{p}_5, \dot{p}_6) &= 0 \end{aligned} \tag{40}$$

Substitution of (40) in Table 2 and the results in (8) for L_{11} leads to

$$\dot{\lambda} = 0.375\ \dot{u} - 0.182\dot{v} \tag{41}$$

Equations (40) and (41) with $\dot{v} = 0$ can then be substituted in Table 2 to give explicit expressions for the stress rates. This stage terminates when the displacement prescription changes at $\Delta u_E = 0.195$, with results given on the lines 2.2 in Tables 3 and 4.

Stage 3 with $\dot{u} = \dot{v}$ is also divided into two parts. In stage 3.1, triangle 1 remains on L_{11} until $f_1 = 1$ again for $\Delta u_F = 1.511$ which leads to the new tangent plane

$$L_{12} = 0.964Q_1 - 0.367Q_2 - 0.697Q_3 = 1 \tag{42a}$$

and backtracking shows that the stage ends at $\Delta u = 0.730$. In stage 3.2, triangle 1 leaves L_{11} but stays on L_{12} until stage 3 terminates with $\Delta u_E = 1.520$.

Stage 4, in which v is increased to 4.5 with u held constant at 4.5,

begins with triangle 1 leaving L_{12}, so that the entire plate is elastic. Now $f_2 = 1$ becomes the violated condition, and in stage 4.2 triangle 2 is on the tangent plane

$$L_{21} = 1.030Q_4 - 0.679Q_5 - 0.185Q_6 = 1 \tag{42b}$$

In stage 5, v increases from 4.5 to 9.0 and $\dot{u} = -\dot{v}$. There are four substages as triangle 2 unloads elastically, but triangle 1 repeatedly encounters $f_1 = 1$. Thus, stage 5.1 is elastic, and in stages 5.2, 5.3, and 5.4, triangle 1 is respectively, on

$$L_{13} = 0.114Q_1 - 0.287Q_2 + 1.753Q_3 = 1 \tag{42c}$$

$$L_{14} = -0.211Q_1 - 0.065Q_2 + 1.753Q_3 = 1 \tag{42d}$$

$$L_{15} = -0.521Q_1 + 0.136Q_2 + 1.564Q_3 = 1 \tag{42e}$$

Thus far we have not mentioned symmetry or isotropy. Whenever one yield flat is formed, one may wish to immediately introduce various symmetric linear constraints. Thus, if the loading has established

$$L = a\sigma_x + b\sigma_y + c\tau = 1 \tag{43}$$

as a linear yield condition, one has the option of immediately defining any of

$$L' = -a\sigma_x - b\sigma_y - c\tau = 1 \tag{44a}$$

$$L'' = a\sigma_x + b\sigma_y - c\tau = 1 \tag{44b}$$

$$L''' = -a\sigma_x + b\sigma_y + c\tau = 1 \tag{44c}$$

$$L'''' = b\sigma_x + a\sigma_y + c\tau = 1 \tag{44d}$$

representing, respectively, complete symmetry in tension-compression, shear symmetry, symmetry of σ_x in tension-compression, and isotropy. If more than

one of (44) are used they will obviously combine to give further combinations.

To illustrate the application of this idea, we shall adopt only (44a) so that for each yield flat L_{kj} defined by (30) or (42), another flat $L'_{kj} = - L_{kj}$ is also defined.

These additional yield flats first become relevant during stage 6 in which v = 9.0 and t = -u is increased from 0 to 9.0. In stage 6.1, triangle 1 remains on L_{15} and at $\Delta t_F = 2.275$, $f_1 = 1$ again. However, at $\Delta t_L = 1.336$, triangle 1 encounters flat L'_{11}, i.e., L_{11} as given by Eq. (39) takes on the value -1. Stages 6.2 and 6.3 find triangle 1 on L'_{11} and L'_{12}, respectively, but then the surface $f_1 = 1$ is encountered again and a new flat

$$L_{16} = -0.887Q_1+0.053Q_2+0.595Q_3 = 1 \tag{45}$$

is defined.

In stage 6.4, triangle 1 remains on both L'_{12} and L_{16}, but since three stresses are involved this does not necessarily correspond to a constant stress. Instead, the plastic strain rates must be written

$$\begin{aligned}(\dot{p}_1,\dot{p}_2,\dot{p}_3) = \dot{\lambda}_1(-0.964,0.367,0.697) \\ + \dot{\lambda}_2(-0.887,0.053,0.595)\end{aligned} \tag{46}$$

and the two additional equations $\dot{L}_{16} = \dot{L}'_{12} = 0$ solved simultaneously to yield

$$\dot{\lambda}_1 = 0.033\dot{t} \qquad \dot{\lambda}_2 = 0.421\dot{t} \tag{47}$$

Substitution of (46) and (47) in Table 2 then leads to the stress rates.

Stage 6.4 ends when triangle 2 encounters flat L'_{21}. In the next stage, L'_{12}, L_{16}, and L'_{21} are all active. In a load-controlled test, activation of three yield planes would generally cause collapse with all $\dot{Q}_i = 0$, but this solution is not consistent with $\dot{v} = 0$. Instead, (46) must be used, together

with

$$(\dot{P}_4,\dot{P}_5,\dot{P}_6) = \dot{\mu}(-1.030,0.679,0.185) \tag{48}$$

and $\dot{L}'_{12} = \dot{L}_{16} = \dot{L}'_{21} = 0$ to obtain

$$\dot{\lambda}_1 = 0.256\dot{t} \quad \dot{\lambda}_2 = 0.122\dot{t} \quad \dot{\mu} = 0.143\dot{t} \tag{49}$$

whence Table 2 again provides the stress rates. Stage 6.5 terminates when $u = -9.0$.

In stage 7, $u = v = -t$. It turns out that under this loading triangle 1 leaves L_{16} but remains on L'_{12}, and triangle 2 remains on L'_{21}. This stage is to continue until $P_y = Q_3/2 = 0$ which leads to $\Delta t_E = 3.926$. However, triangle 1 hits a new portion of $f_1 = 1$ at $\Delta t_F = 2.692$, whence stage 7.1 ends with formation of

$$L_{17} = -1.047Q_1 + 0.470Q_2 + 0.153Q_3 = 1 \tag{50}$$

and $\Delta t = 0.937$. Flats L_{17} and L'_{21} are the active ones in stage 7.2 and this time the external condition $Q_3 = 0$ governs the end of the stage.

Stage 8 is a load controlled one, so it is convenient to solve the first and third equations in Table 2 for $\dot{u}$ and $\dot{v}$ in terms of $\dot{P}_x$ (and $\dot{P}_y = 0$). When the results are substituted in the remaining equations in Table 2, explicit dependence on $\dot{p}_1$ and $\dot{p}_3$ disappears, and the resulting stress equations can be simply written in terms of the parameters

$$\dot{t} = 0.08\dot{P}_x/\sigma_o$$

$$\dot{r} = -0.06(\dot{p}_4+\dot{p}_5+\dot{p}_6)+0.52(\dot{p}_5-\dot{p}_2) \tag{51}$$

$$\dot{s} = -0.18(\dot{p}_4+\dot{p}_5+\dot{p}_6)+0.06(\dot{p}_5-\dot{p}_2)$$

the results being

$$\dot{Q}_1 = 25\dot{t} \qquad \dot{Q}_2 = -\dot{t}+\dot{r} \qquad \dot{Q}_3 = 0$$

$$\dot{Q}_4 = 22\dot{t}+\dot{s} \qquad \dot{Q}_5 = 2\dot{t}-\dot{r}+\dot{s} \qquad \dot{Q}_6 = -3\dot{t}+\dot{s} \tag{52}$$

$$\dot{Q}_7 = \dot{Q}_8 = -(1/2)\dot{Q}_6$$

All triangles are elastic in stage 8.1, which terminates when triangle 1 encounters L'_{17}, and remains there until collapse. Triangle 2 is still elastic in stage 8.2, but returns to L_{21}, (Eq. 42b) for stage 8.3. The limiting condition for stage 8.3 is $f_2 = 1$ which leads to the final plane

$$L_{22} = 0.932Q_4-0.684Q_5-0.725Q_6 = 1 \tag{53}$$

Collapse now occurs, since $\dot{Q}_i = 0$ is the unique solution of Eqs. (52) and $\dot{L}'_{17} = \dot{L}_{21} = \dot{L}_{22} = 0$, and all three plastic multipliers are positive.

At each substage of the solution, the plastic strain rates are obtained, and a running record is kept of their accumulated values in Table 4. However, Eqs. (34) and (35) give the displacements and strains in finite form, so that they are easily computed from Tables 3 and 4 whenever they are desired. During the deformation-controlled process, the loads are given by (37), and when loads are controlled tip deformations are given by (34b).

It is of some interest to compare the preceding solution with an unadjusted use of the Mises yield condition using approximately the same number of time steps. In this analysis, the limit and end of a step is either Δt_E, or Δt_F when an elastic triangle reaches the current yield value f_i°. When f_i° has been reached plastic flow will take place along the tangent plane to the surface $f_i = f_i^\circ$ so that at the end of the step the value of f_i° must be recomputed as the then current value of f_i. For a fair comparison, stages 2 and 4 each consist of one elastic and one plastic step, stage 3 is divided into two steps

with $\Delta u = 1.125$ and stage 5 consists of an elastic step followed by three plastic steps with equal Δv. Stage 6 is first subdivided into five steps with $-\Delta u = 1.80$ in each, but the last step is further split in two by triangle 2 becoming plastic. Stage 7 is taken in equal steps of $\Delta u = -2.5$, and it is found that $P_y = 0$ part way through the second step. The first step in stage 8 is elastic until triangle 2 becomes plastic. Step 8.2 is terminated by triangle 1 becoming plastic and subsequent steps are chosen so that $\Delta\lambda$, the integrated plastic strain multiplier for triangle 1 is equal to 1.00. It is found that the load does not increase significantly after the end of 8.2, but a collapse mechanism occurs only at the end of stage 8.5. Values of stress and plastic strain according to this analysis are presented in Tables 5 and 6. Table 6 also shows the current yield values. By the end of the loading, because of finite motion on tangent planes, the yield value for triangle 2 has increased 10%, and for triangle it has increased 67%.

Figure 7 gives a pictorial history of the load and tip deformation. The deformation histories are prescribed through the first 7 stages, but differ noticeably during the final increase of P_x, wheras the load histories gradually diverge through the first 7 stages and show a 25% difference in the predicted collapse loads. The light ellipse in Fig. 7 is an upper bound on the yield-point interaction curve, corresponding to plastic deformation of only triangle 1. The unadjusted analysis predicts loads in excess of collapse from stage 5.1 through stage 7, and also for the final collapse load.

Figure 8 presents the same information from a different viewpoint as a load-deformation diagram in the horizontal direction. Figure 9 gives an exaggerated view of the total deformation at the end of stage 6. Although the tip deformation, being prescribed, is the same for both theories, the strains and other nodal deformations are measurably different between the two.

6. Conclusions A method has been described and illustrated for automatic piecewise linearization of finite element analyses for linearly-elastic/perfectly-plastic structures. According to the method, material behavior is originally described by a nonlinear outer yield surface and a related inner yield surface. As the loading progresses, yield flats are formed which are linear constraints lying wholly between the two surfaces. Therefore, at any instant, the current yield condition consists of any number of yield flats plus, possibly, a portion of the original outer surface, Although the current condition may change, at any instant it is fully contained within the yield condition at any previous instant.

The examples were purposely chosen to be very small in order to clearly illustrate the principles involved. In implementing the procedure for large scale problems, various refinements might be considered.

The use of symmetry and isotropy to more rapidly create linear yield flats has already been commented on in Section 5. It should be pointed out that isotropy is used in a very limited sense. If the principal stress directions are variable, then no piecewise linear yield function can be fully isotropic, since a general rotation of axes transforms a linear function into a non-linear one. The isotropy referred to amounts only to interchange of fixed coordinate axes or, equivalently, to rotations which are multiples of 90°.

Another possible refinement is to use the same piecewise linearization with respect to all elements. This would obviously reduce storage requirements. A minor problem would exist if the stress point for element 2, say, was between the inner and outer yield curves, but fell outside of a yield flat newly created by element 1. However, this aspect could easily be handled by a method similar to the loss of ancient history problem as at point M in Fig. 1d.

In order to reduce the number of time steps, it might be desirable to examine all elements when a stage is terminated, and to construct yield flats for any whose stress points are outside the inner curve, even if they are not yet on the outer curve.

Two drawbacks to the procedure should be noted. First, if two or more problems are solved for the same structure as part of the same program so that each problem starts with any yield flats developed from previous ones, then the solutions may differ depending upon the order of solution. Second, a stress point strictly between the two curves may be reached early in the loading history which is outside of a flat established later. It is even possible that such a point could correspond to plastic collapse of the structure according to the final yield criterion. Although either of these situations is theoretically embarrassing they should not prove to be of great practical significance, since the current yield condition is always bounded by the original inner and outer surfaces which can be chosen to be reasonably close to each other.

The method is readily adaptable to strain-hardening, and, indeed, might be somewhat simpler to apply. For a strain-hardening material, let the initial yield condition for an elastic element be the inner yield curve, and terminate the elastic stage when this limit is reached as at point C in Fig. 10.

Construct the yield flat JCD and assume loading continues on this flat according to whatever hardening law is being used. During this stage the current yield condition consists of the flat JCD together with that portion of the outer yield curve which has not been cut off by JCD. If, for example, the hardening is isotropic, this entire configuration would expand as the stress point moved outside the original flat JCD. This phenomenon is easily incorporated into Fig. 10 by letting the stress scale shrink to account for

the hardening. Similarly, if the hardening is kinematic, the stress origin can be moved.

If the stress point reaches D (in its new, hardened position), then the shrink and backtrack technique is used just as in perfectly plasticity to form a new flat ENK.

If unloading occurs at point F, the behavior will be elastic and the current yield condition consists of the existing flats JCD and ENK, the inner yield curve QIT which is not influenced by the flats, and conical portions such as AQK connecting these two. Note that this surface is not convex.

Plastic flow may recommence in three different manners. For trajectory FGI it will start with formation of a new tangent flat at I. For trajectory FGH, the inner yield curve is inoperative and plastic flow recommences at H according to the existing flat JCD.

However, if the unloading trajectory encounters the conical portion of the yield condition as at P, then the shrink and backtrack technique must be used to create the new yield flat RQU. With this method, although the limiting elastic condition during elastic behavior may be non-convex, the yield condition during plastic flow will always be convex. For example, regarding Fig. 10 as two-dimensional, the stress trajectory ABCEFG produces the non-convex elastic limit consisting of straight line segments TJ, JE, EK, KQ and the circular arc QIT, wheras the trajectory ABCERS produces the convex yield condition consisting of straight lines JE, ER, RU and the circular arc ULJ. An application of this procedure to a plasticity problem with strain hardening will be presented elsewhere.

REFERENCES

1. P. G. Hodge, Jr., T. Belytschko, and C. T. Herakovich: Quadratic programming and plasticity, "Computation Approaches in Applied Mechanics," E. Sevin, Ed., American Society of Mechanical Engineers, New York, 1969, pp. 73-84.

2. P. G. Hodge, Jr.: Computer solutions of plasticity problems, " Problems of Plasticity," Vol. 2, A. Sawczuk, Ed., Noordhoff International Publishing, Leyden, 1974, pp. 261-282.

3. H. Tresca: Mémoire sur l'écoulement des corps solides, Mém. prés. par div. sav. 18, 733-799 (1868).

4. R. von Mises: Mechanik der festen Korper in plastisch deformablen Zustand, Nachr., Gottingen Akad. wiss. Math.-physik. Kl., 1913, 582-592 (1913).

5. P. G. Hodge, Jr.: Finite element methods in plasticity: Proc. 7th U.S. Nat. Congr. Appl. Mech. S. K. Datta, ed. (Boulder 1974), ASME, 1974, pp. 114-119.

6. D. C. Drucker, Plasticity of metals - mathematical theory and structural applications, Trans. ASCE, 116, 1059-1072 (1951).

End of Stage	Load x 100	Displacements x 100		Generalized stresses x 100					
				element 1		element 2		element 3	
	p	ϕ	δ	n_1	m_1	n_2	m_2	n_3	m_3
1	1017	50	186	86	- 17	339	- 17	592	-17
2	1183	57	217	96	-0.4	402	- 19	685	-19
3	2081	↓	397	↓	↓	851	- 19	1134	-19
4	2106	61	409	92	-2	869	- 20	1144	0.3
5	2435	191	734	-68	-45	1358	- 63		
6	2461	206	766	-81	-26	1398	- 69		
7	2486	226	801	-95	-0.7	1437	- 75		
8	2548	2092	2792	↓	↓	1499	-697		

Table 1: Truss results

Stress rate	$\frac{3\dot{u}}{1120}$	$\frac{3\dot{v}}{1120}$	$\frac{3\dot{p}_1}{560}$	$\frac{\dot{p}_2}{560}$	$\frac{3\dot{p}_3}{560}$	$\frac{3\dot{p}_4}{560}$	$\frac{\dot{p}_5}{560}$	$\frac{3\dot{p}_6}{560}$
$\dot{Q}_1/2$	58	-13	-58	-18	13	-37	3	8
$\dot{Q}_2/2$	6	-11	- 6	-166	11	1	121	-4
$\dot{Q}_3/2$	-13	18	13	33	-18	- 8	12	-3
$\dot{Q}_4/2$	37	8	-37	3	- 8	-58	-18	-13
$\dot{Q}_5/2$	- 1	- 4	1	121	4	- 6	-166	-11
$\dot{Q}_6/2$	- 8	3	8	-12	- 3	-13	-33	-18
$\dot{Q}_7/21$	1	- 1	- 1	- 1	1	1	1	1
$\dot{Q}_8/5$	- 1	3	1	9	- 3	1	9	3

Table 2: Stress rate equations for triangular plate.

End of Stage	Displacement x 100		Stress x 100							
			triangle 1			triangle 2			triangle 3	
	u	v	Q_1	Q_2	Q_3	Q_4	Q_5	Q_6	Q_7	Q_8
1	0	-225	16	13	-22	-10	5	-4	13	9
2.1	205	↓	80	20	-36	31	4	-12	24	-12
.2	225	↓	81	20	-35	33	3	-12	24	-11
3.1	298	-152	90	17	-29	48	-1	-13	21	- 8
.2	450	0	99	16	-16	71	-13	-12	14	- 2
4.1	↓	282	79	0	12	83	-19	- 7	- 2	10
.2	↓	450	63	-13	27	84	-18	- 5	-11	16
5.1	295	605	4	-27	52	60	-21	4	-28	24
.2	230	670	-16	-24	54	45	-23	7	-31	24
.3	89	811	-43	-19	51	18	-22	10	-31	20
.4	0	900	-51	-20	49	8	-18	11	-30	19
6.1	-134	↓	-70	-18	42	-15	-12	12	-27	15
.2	-440	↓	-92	-22	28	-52	6	12	-20	8
.3	-587	↓	-98	-32	25	-62	18	11	-18	7
.4	-866	↓	-104	-30	15	-78	26	11	-13	2
.5	-900	↓	-104	-30	15	-78	26	11	-13	2
7.1	-994	806	-104	-22	12	-80	22	12	-12	0
.2	-1400	400	-98	- 3	0	-83	17	14	- 7	-7
8.1	-679	921	91	-11	0	82	3	-9	4	4
.2	-536	954	97	3	0	89	-10	-8	4	4
.3	773	1719	97	4	0	82	-18	-15	7	7

Table 3: Tip displacements and stresses.

End of Stage	Plastic displacement x 100					
	triangle 1			triangle 2		
	p_1	p_2	p_3	p_4	p_5	p_6
2.1	0	0	0	0	0	0
2	6	-2	-9	↓	↓	↓
3.1	17	-5	-25			
2	56	-20	-54			
4.2	↓	↓	↓	12	-8	-2
5.2	59	-27	- 9	↓	↓	↓
3	44	-32	114			
4	19	-25	190			
6.1	- 4	-19	258			
2	-94	7	392			
3	-155	31	437			
4	-264	40	510			
5	-276	43	519	7	-4	-1
7.1	-293	50	531	-20	13	4
2	-395	96	546	-120	79	22
8.2	-336	69	537	↓	↓	↓
3	62	-109	479	140	-92	-25

Table 4: Plastic strains.

End of Stage	Displacement x 100		Stress x 100							
			triangle 1			triangle 2			triangle 3	
	u	v	Q_1	Q_2	Q_3	Q_4	Q_5	Q_6	Q_7	Q_8
1	0	-225	16	13	-22	-10	5	- 4	13	9
2.1	222	|	85	20	-37	34	4	-13	25	-12
2	225	↓	85	20	-37	35	3	-13	25	-12
3.1	338	-112	98	16	-27	57	- 3	-14	20	- 7
2	450	0	107	14	-17	76	-10	-13	15	- 2
4.1	|	311	85	-4	13	89	-17	- 8	- 2	10
2	↓	450	71	-15	25	90	-17	- 6	- 9	16
5.1	254	646	- 3	-32	58	60	-20	5	-32	26
2	169	731	-30	-28	60	40	-23	9	-35	26
3	85	815	-48	-24	59	23	-24	12	-35	24
4	0	900	-60	-22	57	9	-22	13	-35	22
6.1	-180	|	-87	-18	49	-23	-16	15	-32	17
2	-360	|	-104	-20	40	-48	- 5	16	-28	12
3	-540	|	-115	-25	33	-67	7	15	-24	9
4	-720	|	-123	-31	27	-82	19	14	-20	6
5	-758	|	-124	-33	25	-84	22	14	-20	6
6	-900	↓	-124	-33	25	-85	21	14	-20	6
7.1	-1150	650	-124	- 8	16	-95	6	14	-15	1
2	-1674	126	-117	22	0	-102	- 8	15	- 7	- 7
8.1	- 857	716	96	14	0	85	-25	-11	5	5
2	- 595	1002	119	-19	0	102	2	-17	8	8
3	- 15	1484	119	-19	0	101	2	-17	8	8
4	564	1964	119	-19	0	101	2	-17	8	8
5	1144	2444	119	-19	0	101	2	-17	8	8

Table 5: Unadjusted plate stresses.

End of Stage	Plastic strains x 100						Yield value x 100	
	Triangle 1			Triangle 2				
	p_1	p_2	p_3	p_4	p_5	p_6	f_1°	f_2°
2.1	0	0	0	0	0	0	100	100
2	1	-0.3	-1	↓	↓	↓	100^+	↓
3.1	18	-5	-27	↓	↓	↓	105	↓
2	44	-15	-50	↓	↓	↓	109	↓
4.2	↓	↓	↓	9	-6	-2	↓	100.1
5.2	48	-25	5	↓	↓	↓	118	↓
3	42	-30	77	↓	↓	↓	122	↓
4	26	-30	152	↓	↓	↓	124	↓
6.1	0	-25	243	↓	↓	↓	135	↓
2	-46	-10	328	↓	↓	↓	139	↓
3	-104	10	402	↓	↓	↓	142	↓
4	-169	31	464	↓	↓	↓	143	↓
5	-184	35	475	↓	↓	↓	143	↓
6	-233	48	510	-11	8	7	143	100.1
7.1	-275	60	539	-82	55	38	152	102
2	-376	105	579	-237	140	104	167	103
8.2	↓	↓	↓	-147	78	74	↓	110
3	-248	27	↓	15	0	-7	167	110
4	-120	-52	↓	176	-78	-90	167	110
5	8	-130	↓	338	-157	-173	167	110

Table 6: Unadjusted plastic strains and yield values.

Fig. 1

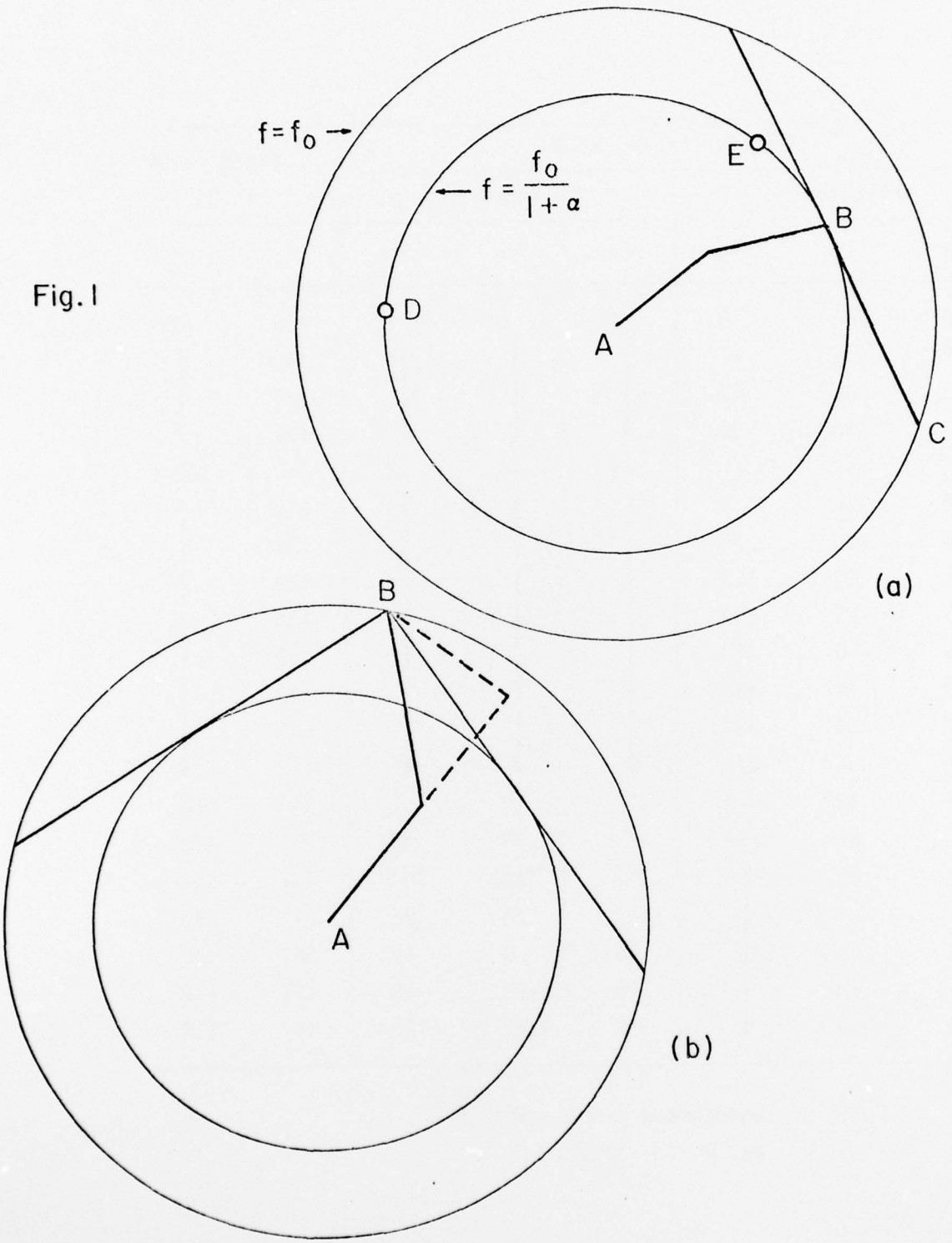

Schematic for piecewise linearization

a. initial tangent

b. external tangent

c. backtrack

d. shrink and backtrack

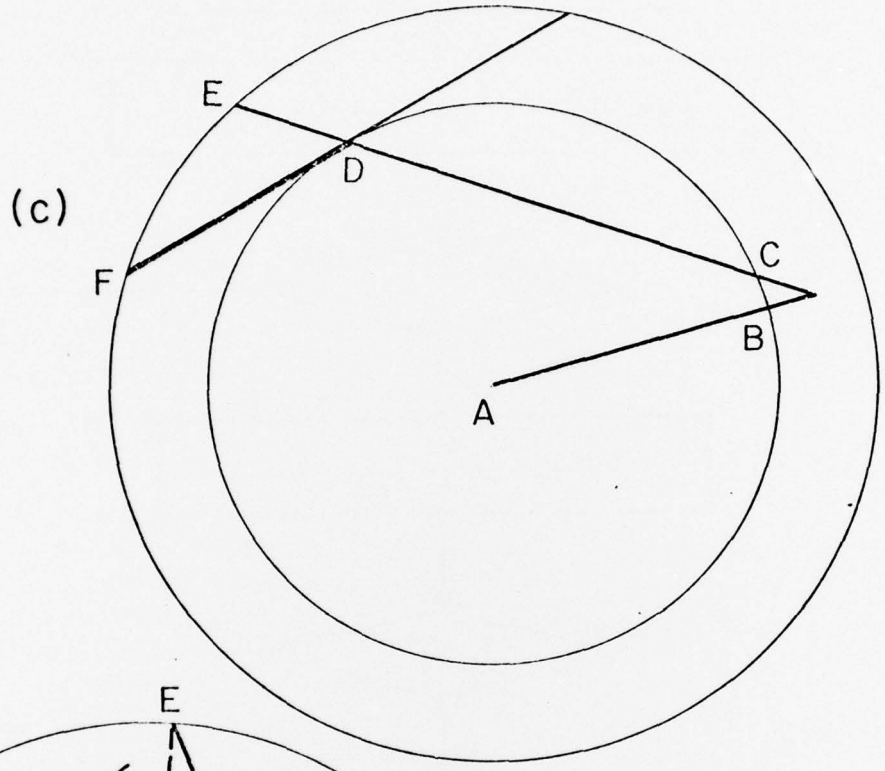

Fig. 1

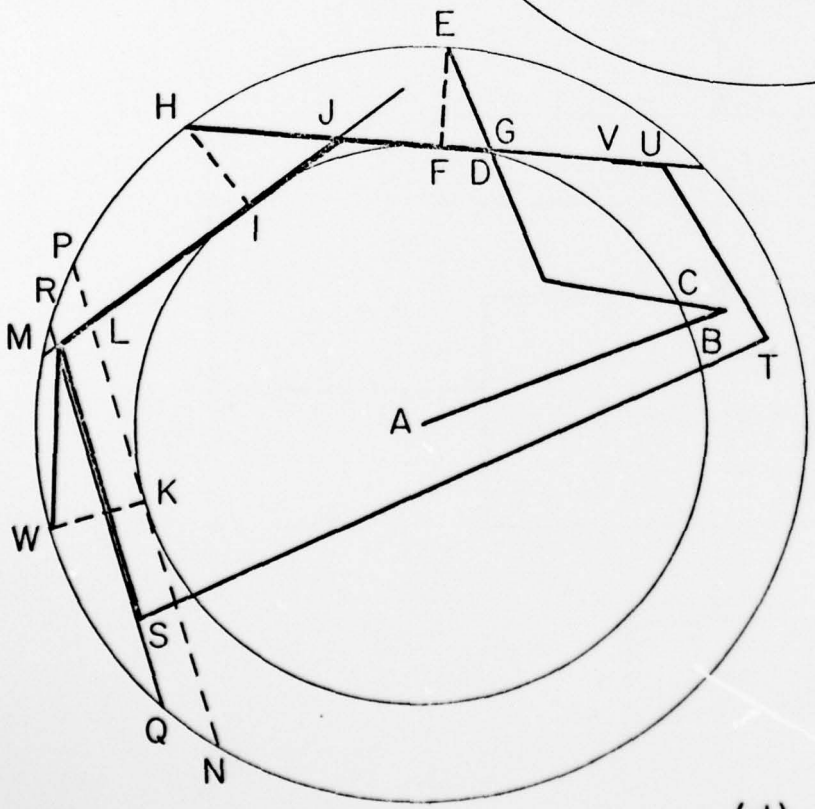

(d)

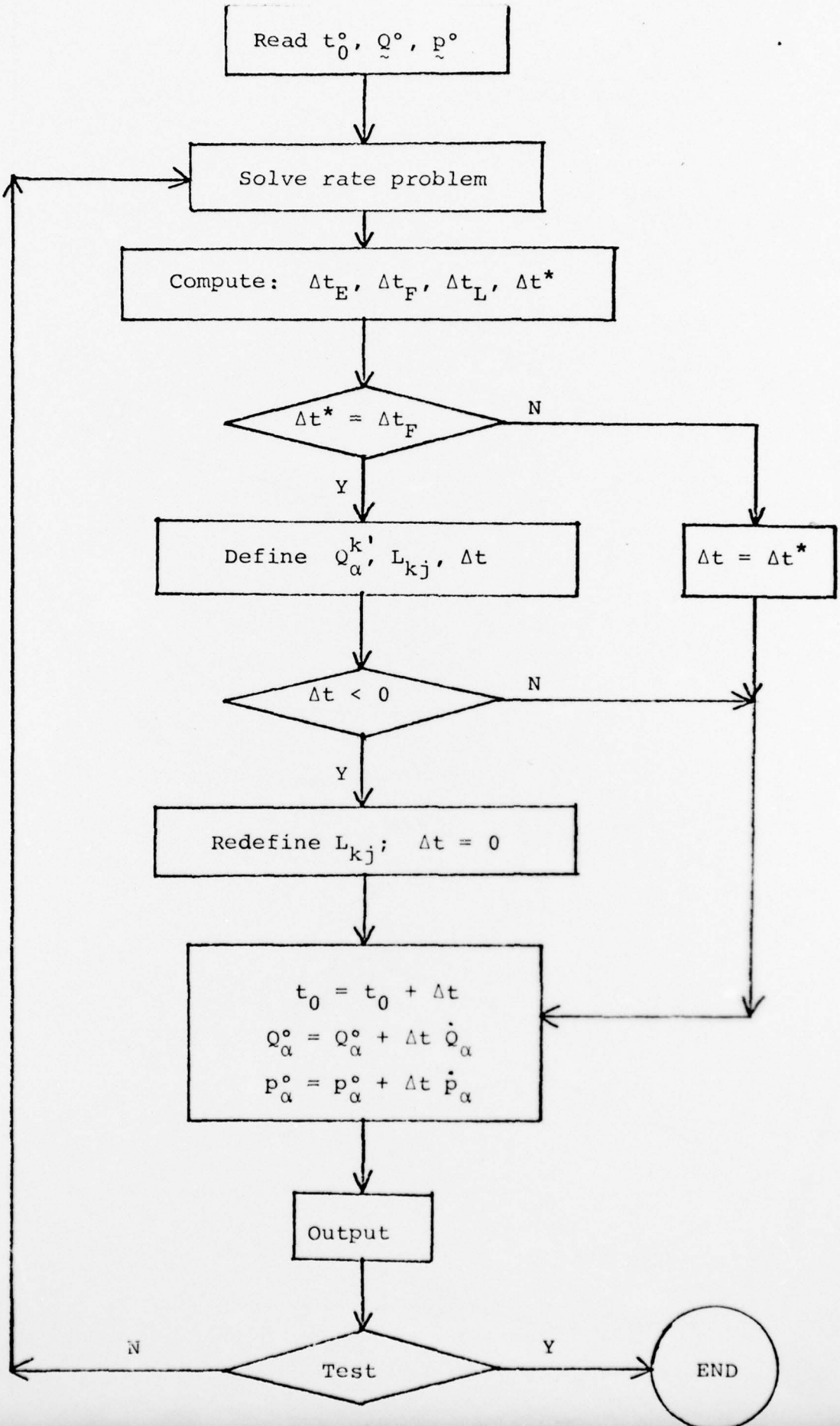
Read t_0°, $\underset{\sim}{Q}^\circ$, $\underset{\sim}{p}^\circ$
Solve rate problem
Compute: Δt_E, Δt_F, Δt_L, Δt^*
$\Delta t^* = \Delta t_F$
N
Y
Define $Q_\alpha^{k'}$, L_{kj}, Δt
$\Delta t = \Delta t^*$
$\Delta t < 0$
N
Y
Redefine L_{kj}; $\Delta t = 0$
$t_0 = t_0 + \Delta t$
$Q_\alpha^\circ = Q_\alpha^\circ + \Delta t\, \dot{Q}_\alpha$
$p_\alpha^\circ = p_\alpha^\circ + \Delta t\, \dot{p}_\alpha$
Output
Test
N
Y
END

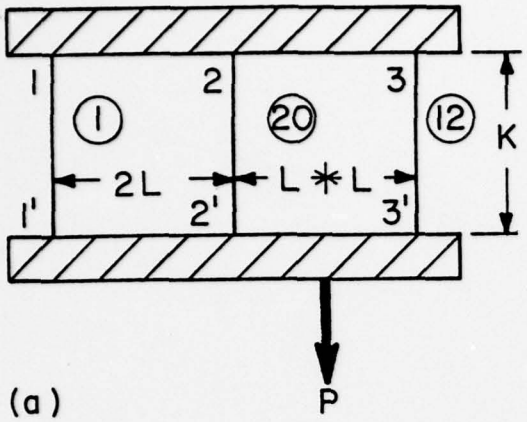

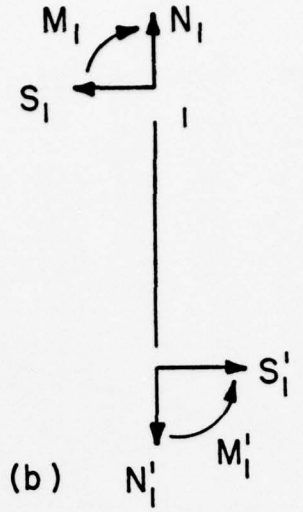

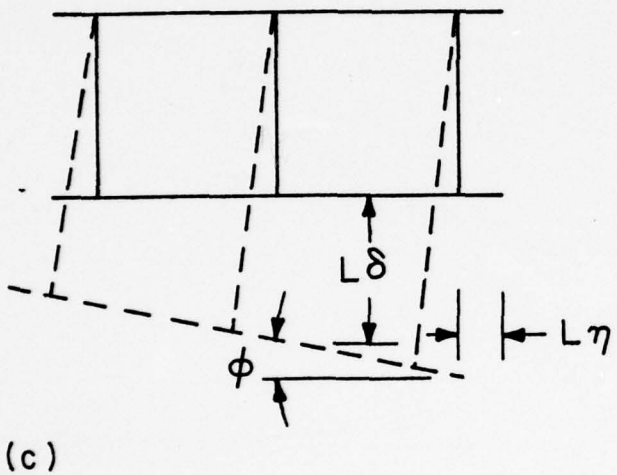

Fig. 3

Three-bar frame

a. Dimensions and yield strengths

b. Stresses

c. Displacements

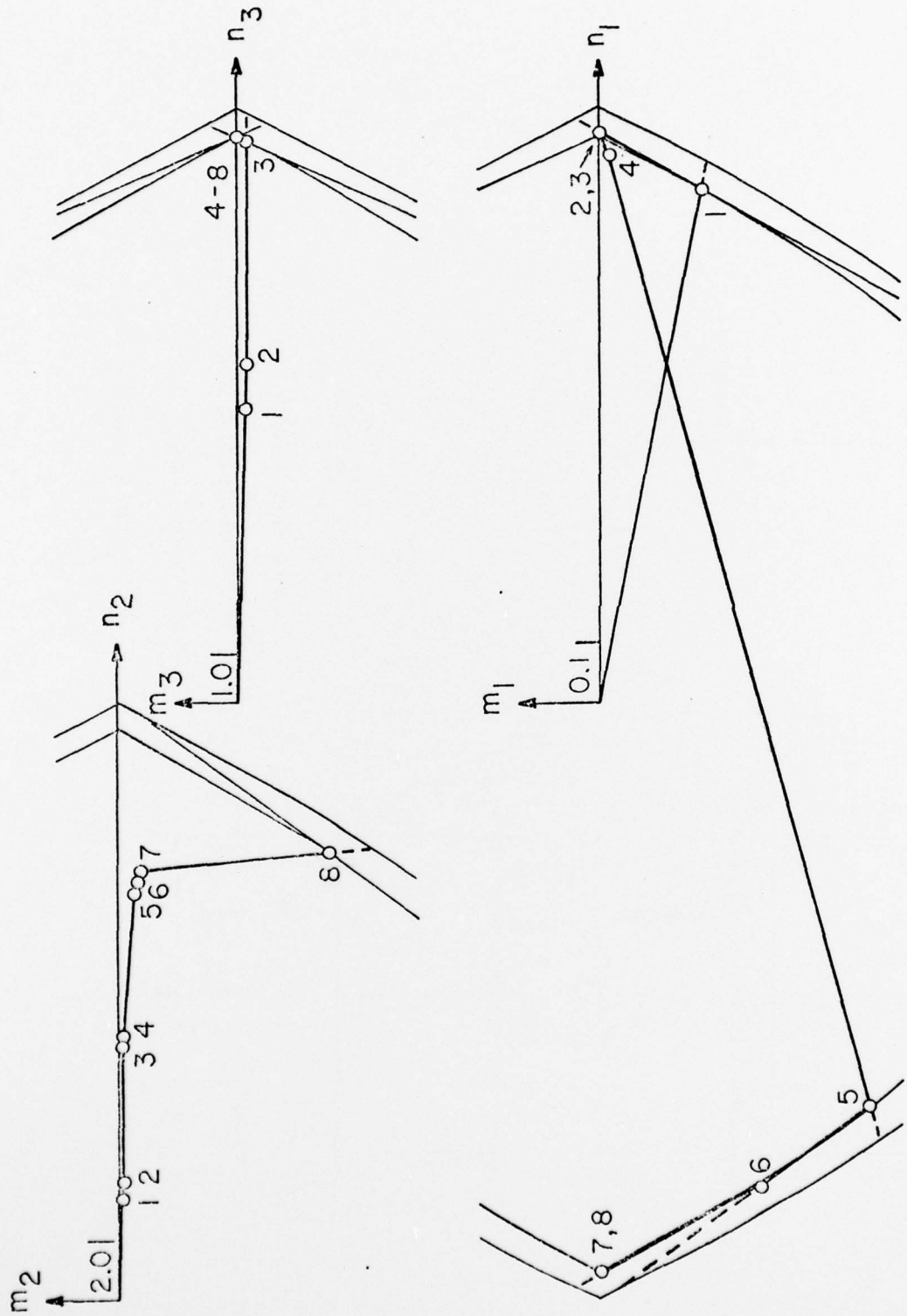

Fig. 4

Stress trajectories for frame

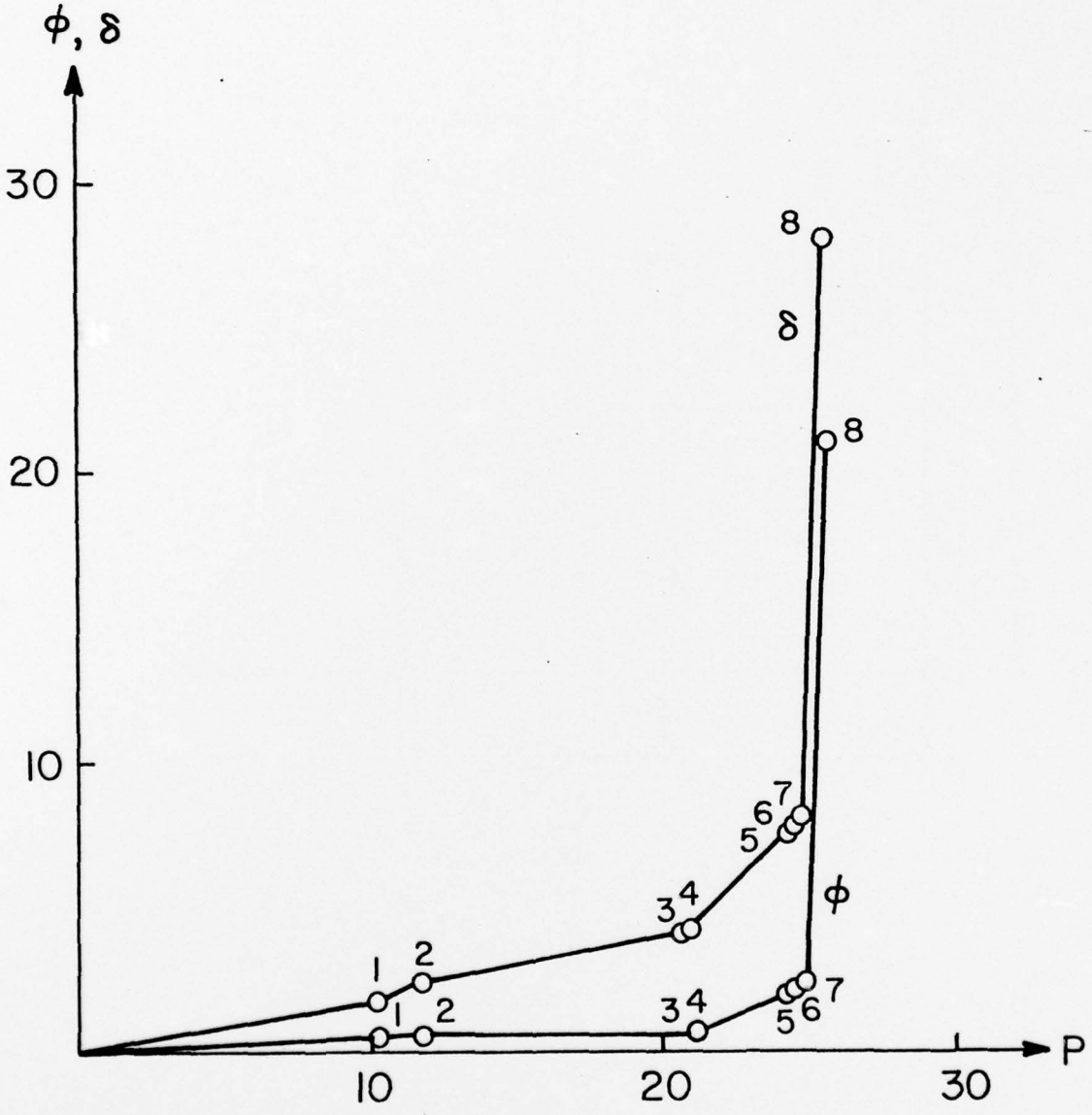

Load-deformation histories for frame

Fig. 5

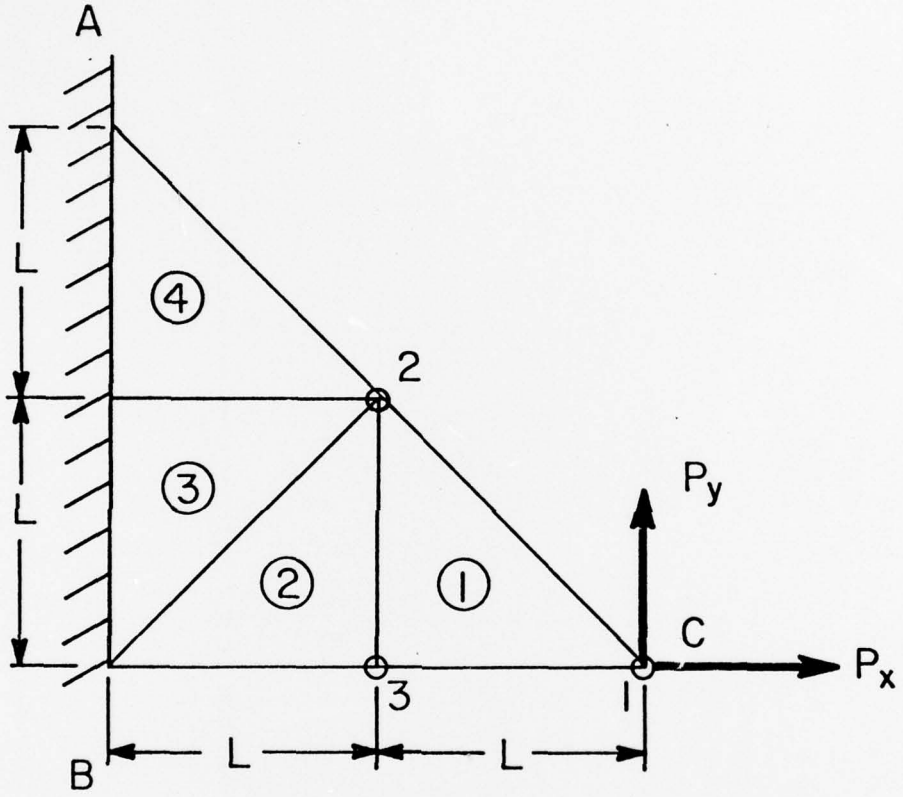

Fig. 6

Triangular plate

Load and tip-deformation trajectories

Fig. 7

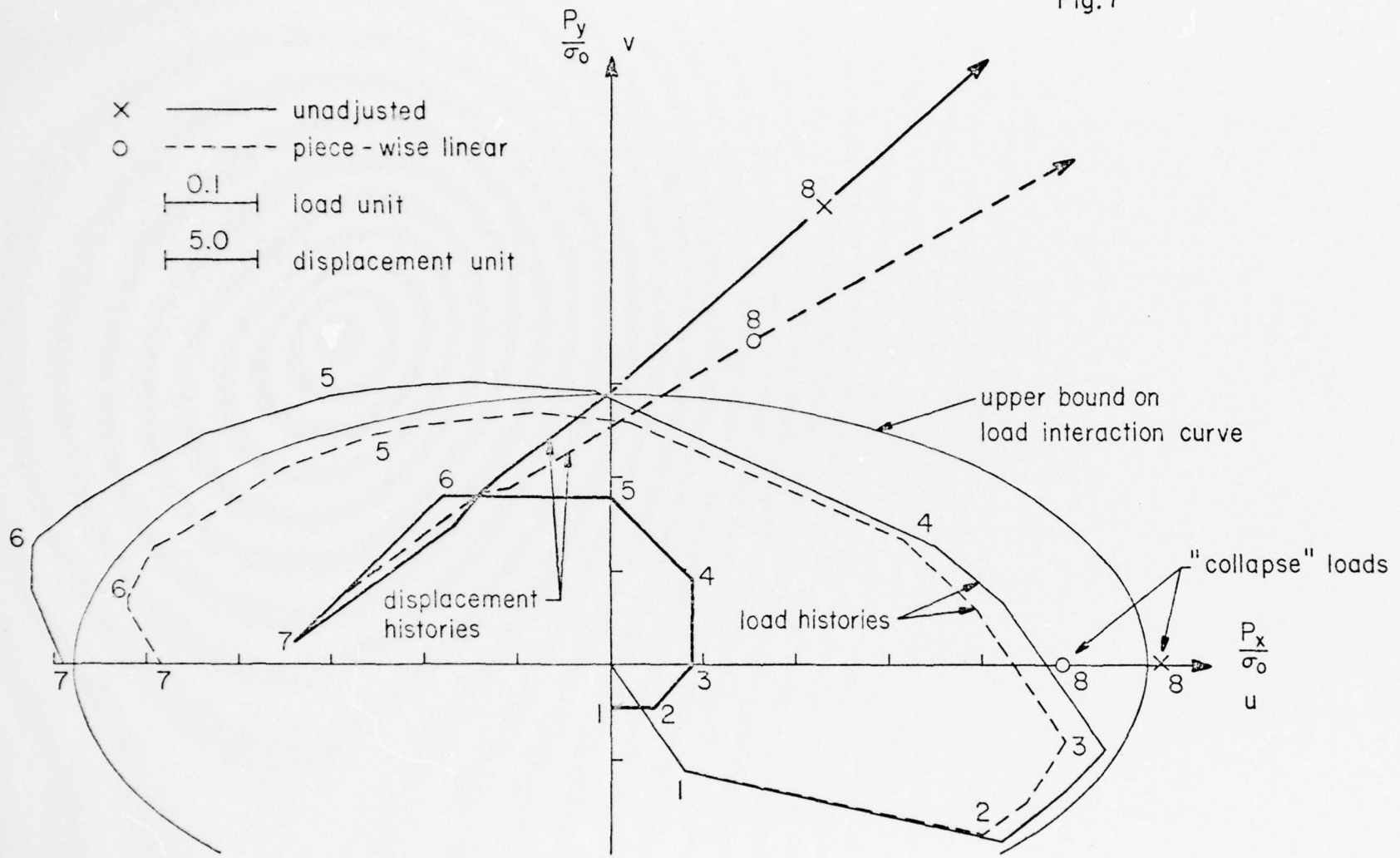

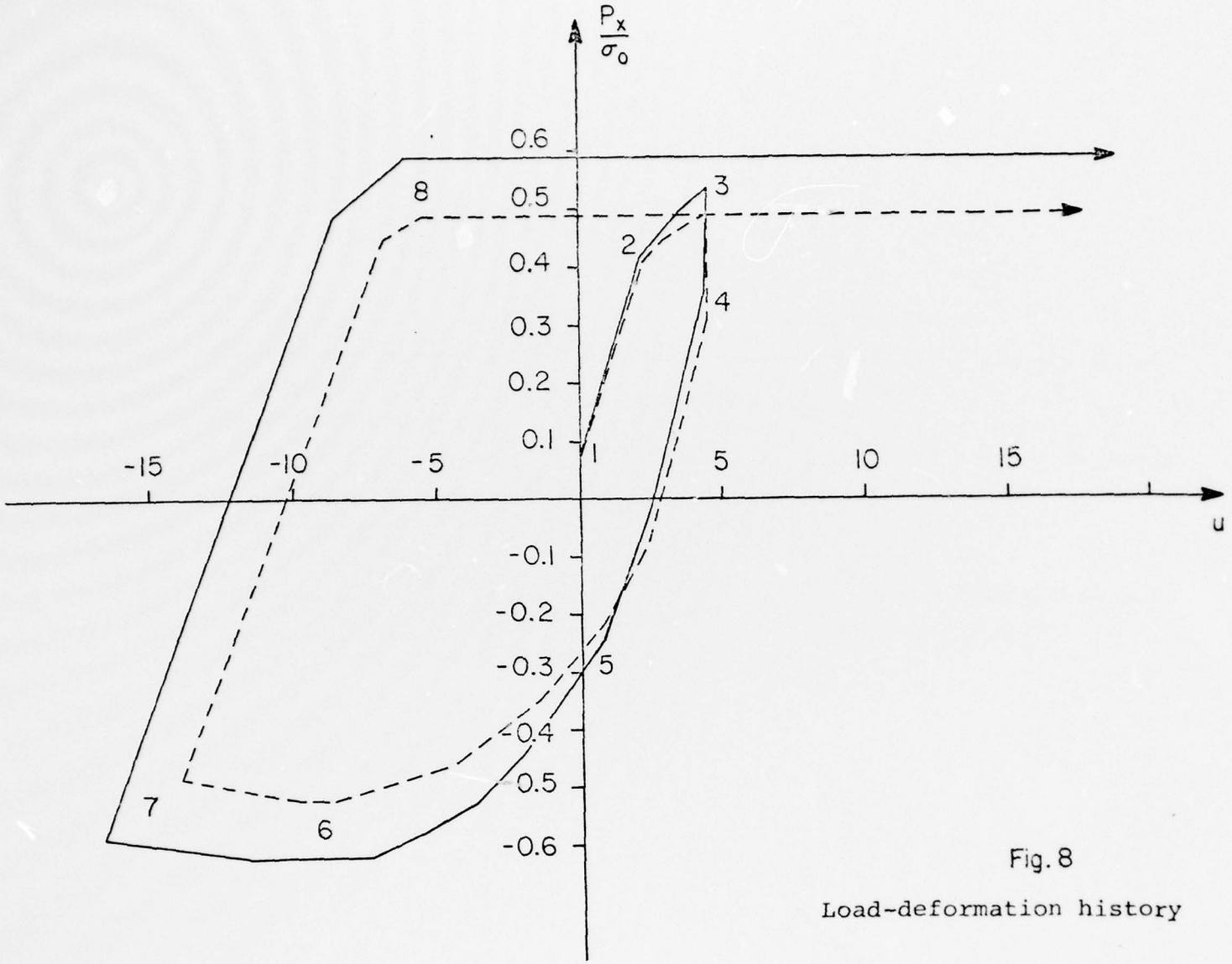

Fig. 8

Load-deformation history

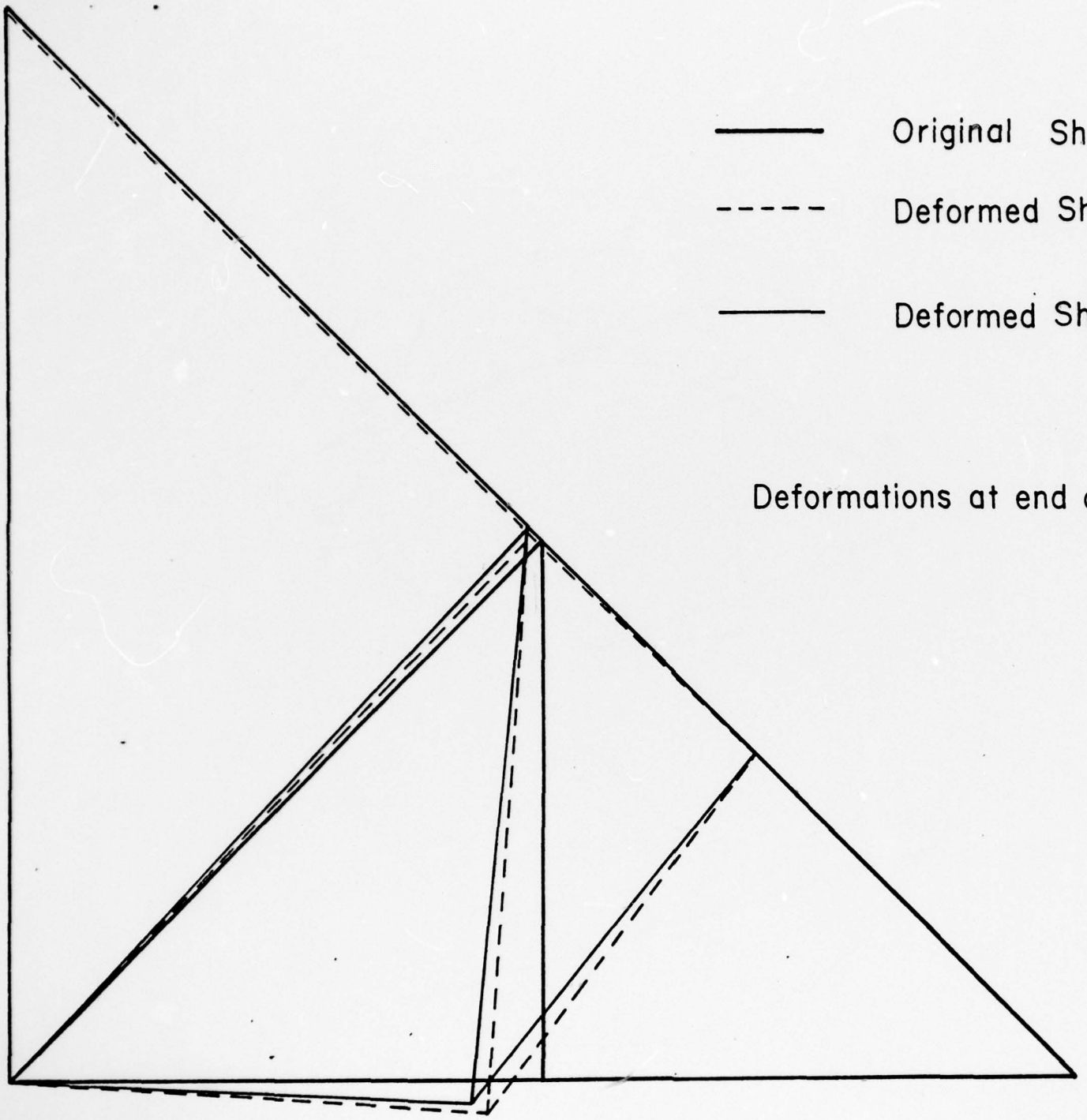

Deformations at end of stage 6.

Fig. 9

Schematic for strain-hardening piecewise linearization

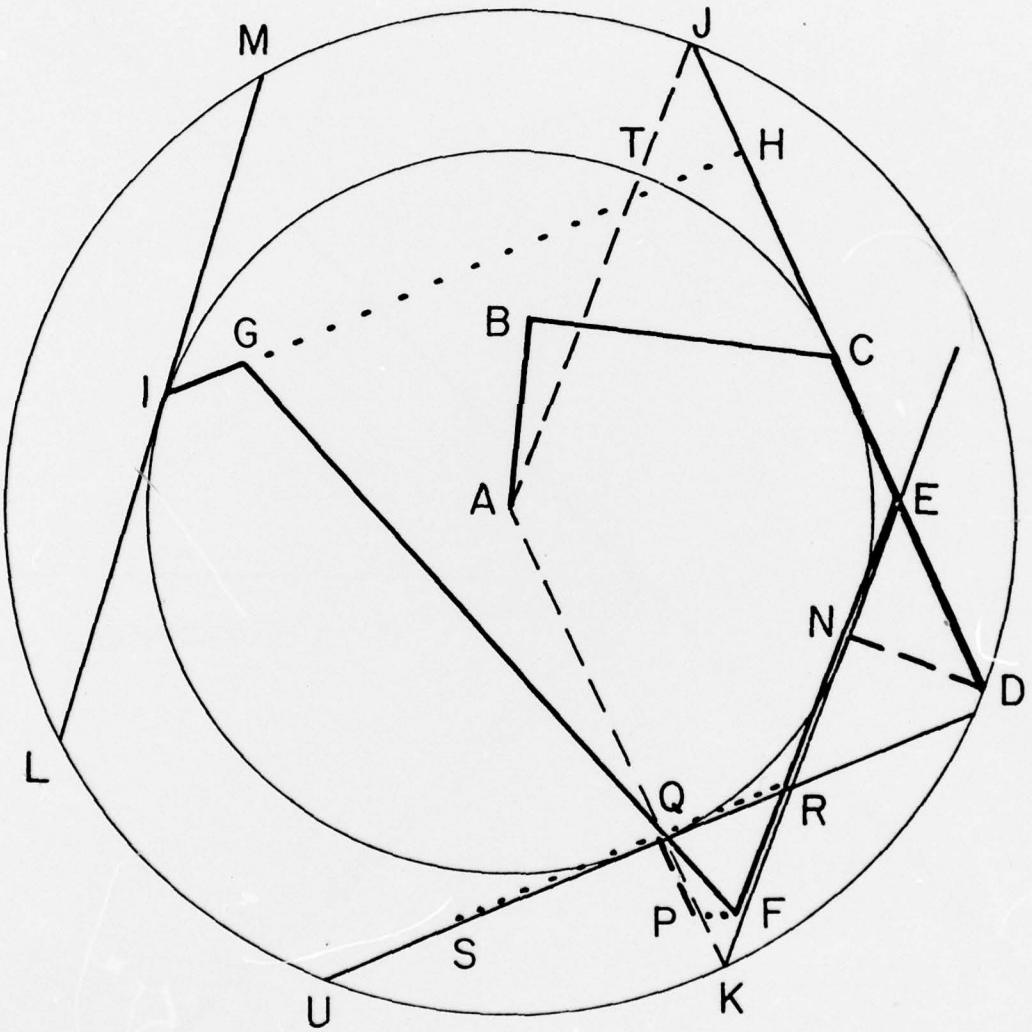

Fig. 10